frontiers | Frontiers in Physics

BRIEF RESEARCH REPORT
published: 20 April 2022
doi: 10.3389/fphy.2022.853717

Elastoresistivity of Heavily Hole-Doped 122 Iron Pnictide Superconductors

Xiaochen Hong[1,2], Steffen Sykora[2,3]*, Federico Caglieris[4,2,5]*, Mahdi Behnami[2], Igor Morozov[2,6], Saicharan Aswartham[2], Vadim Grinenko[2,7,8], Kunihiro Kihou[9], Chul-Ho Lee[9], Bernd Büchner[2,8] and Christian Hess[1,2]**

[1]Fakultät für Mathematik und Naturwissenschaften, Bergische Universität Wuppertal, Wuppertal, Germany, [2]Leibniz-Institute for Solid State and Materials Research (IFW-Dresden), Dresden, Germany, [3]Institute for Theoretical Physics and Würzburg-Dresden Cluster of Excellence ct.qmat, Technische Universität Dresden, Dresden, Germany, [4]Dipartimento di Fisica, University of Genoa, Genoa, Italy, [5]Consiglio Nazionale Delle Ricerche (CNR)-SPIN, Genova, Italy, [6]Department of Chemistry, Lomonosov Moscow State University, Moscow, Russia, [7]Tsung-Dao Lee Institute, Shanghai Jiao Tong University, Shanghai, China, [8]Institute of Solid State and Materials Physics and Würzburg-Dresden Cluster of Excellence ct.qmat, Technische Universität Dresden, Dresden, Germany, [9]National Institute of Advanced Industrial Science and Technology (AIST), Tsukuba, Japan

OPEN ACCESS

Edited by:
Anna Böhmer,
Ruhr-University Bochum, Germany

Reviewed by:
Konrad Jerzy Kapcia,
Adam Mickiewicz University, Poland
Marcin Matusiak,
Institute of Physics (PAN), Poland

***Correspondence:**
Xiaochen Hong
xhong@uni-wuppertal.de
Steffen Sykora
steffen.sykora@tu-dresden.de
Federico Caglieris
federico.caglieris@spin.cnr.it
Christian Hess
c.hess@uni-wuppertal.de

Specialty section:
This article was submitted to Condensed Matter Physics, a section of the journal Frontiers in Physics

Received: *12 January 2022*
Accepted: *21 March 2022*
Published: *20 April 2022*

Citation:
Hong X, Sykora S, Caglieris F, Behnami M, Morozov I, Aswartham S, Grinenko V, Kihou K, Lee C-H, Büchner B and Hess C (2022) Elastoresistivity of Heavily Hole-Doped 122 Iron Pnictide Superconductors. Front. Phys. 10:853717. doi: 10.3389/fphy.2022.853717

Nematicity in heavily hole-doped iron pnictide superconductors remains controversial. Sizeable nematic fluctuations and even nematic orders far from magnetic instability were declared in $RbFe_2As_2$ and its sister compounds. Here, we report a systematic elastoresistance study of a series of isovalent- and electron-doped KFe_2As_2 crystals. We found divergent elastoresistance on cooling for all the crystals along their [110] direction. The amplitude of elastoresistivity diverges if K is substituted with larger ions or if the system is driven toward a Lifshitz transition. However, we conclude that none of them necessarily indicates an independent nematic critical point. Instead, the increased nematicity can be associated with another electronic criticality. In particular, we propose a mechanism for how elastoresistivity is enhanced at a Lifshitz transition.

Keywords: elastoresistance, nematicity, Lifshitz transition, iron-based superconductors, quantum criticality

1 INTRODUCTION

The "122" family, an abbreviation coined for $BaFe_2As_2$ and its substituted sister compounds, played a central role in the study of iron-based superconductors [1]. Those tetragonal $ThCr_2Si_2$-type structured compounds have the advantage that sizeable single crystals with continuous tunable doping can be prepared in a wide range, which is a crucial merit for the systematic investigation of various ordered states. Within the extended phase diagram of 122 compounds, the heavily hole-doped region, including the end-members $K/Rb/CsFe_2As_2$, is of particular interest. The superconducting transition temperature T_c of $Ba_{1-x}K_xFe_2As_2$ peaks at optimal doping $x = 0.4$ and continuously decreases toward the overdoped (larger x) region. T_c remains finite in the end-member $x = 1$, while a change of the Fermi surface topology (Lifshitz transition) exists around $x = 0.6 \sim 0.8$ [2]. Although the T_c vs. x trend seems to be smooth across the Lifshitz transition, there are quite a lot of things happening here. Vanishing electron pockets for $x > 0.8$ destroy the basis of the interpocket scattering induced-$S\pm$ pairing symmetry which is generally believed as a feature of most iron-based superconductors. As a result, a change in the superconducting gap structure across the Lifshitz transition was observed experimentally [2–4]. Comparable pairing strength at the transition can foster a complex pairing state that breaks the time-reversal symmetry. Such an exotic state was also demonstrated to exist around the Lifshitz transition [5, 6]. Very recently, a so-called "Z_2 metal

state" above T_c at the Lifshitz transition has been unveiled, with an astonishing feature of spontaneous Nernst effect [7].

Electronic nematicity, a strongly correlated electronic state of electrons breaking the underlying rotational symmetry of their lattice but preserving translation symmetry, has been a wave of research in unconventional superconductors, particularly in iron-based superconductors [8, 9]. Consistent experimental efforts have identified nematicity in all the different iron-based superconductor families [10–15], accompanied by theoretical proposals of the intimate relationship between nematicity and superconducting pairing [16–19]. However, according to the previous background, we should not simply extend what is known in the under- and optimal-doped 122s to the over-doped region. Whether nematicity exists and how it develops in this region needs independent censoring.

Indeed, nematicity in the heavily hole-doped 122 turns out to be more elusive. Heavily hole-doped 122s stand out as a featured series because of their peculiar Fermi surface topology, isostructural phase transition, and possible novel pairing symmetries [20–23]. Nematically ordered states were suggested by nuclear magnetic resonance spectroscopy and scanning tunneling microscopy on $CsFe_2As_2$ and $RbFe_2As_2$, and they were found to develop in different wave vectors other than the underdoped 122s [24, 25]. Such a nematic state far away from magnetic ordering challenges the prevailing idea that nematicity is some kind of vestigial order of magnetism [26]. An elastoresistance study further claims that a tantalizing isotropic (or XY-) nematicity is realized in the crossover region from dominating [100] nematicity in $RbFe_2As_2$ to [110] nematicity at the optimal doping [27]. However, many works pointed out that elastoresistance in $K/Rb/CsFe_2As_2$ is actually contributed by the symmetric A_{1g} channel, having little to do with the B_{1g} or B_{2g} channels which are related to nematicity [28, 29]. Overall, the debate is still on for this topic.

In this brief report, we will not touch upon the nature of the possible nematicity of $K/Rb/CsFe_2As_2$. Instead, we confirm phenomenologically the existence of elastoresistance (χ^{er}) in $K/Rb/CsFe_2As_2$ and find that its amplitude diverges exponentially with growing substituted ion size. Moreover, we present χ^{er} data on a series of $Ba_{1-x}K_xFe_2As_2$ crystals crossing the Lifshitz transition. We observe, unexpectedly, a clear enhancement of χ^{er} from both sides of the Lifshitz point. Although a presumptive nematic quantum critical point (QCP) might be of relevance, here we propose a rather more conventional explanation based on a small Fermi pocket effect. Our results add a novel phenomenon to the Lifshitz transition of the $Ba_{1-x}K_xFe_2As_2$ system and highlight another contributing factor of elastoresistance which has been almost ignored so far.

2 EXPERIMENTAL DETAILS

Single crystals of heavily hole-doped $Ba_{1-x}K_xFe_2As_2$ were grown by the self-flux method [30–32]. The actual doping level x was determined by considering their structural parameters and T_c values. Elastoresistance measurements were performed as described in Ref. s [10–12]. Thin stripe-shaped samples were glued on the surface of piezo actuators. The strain gauge were glued on the other side of the piezo actuators to monitor the real strain generated. In most cases, the samples were mounted to let the electric current flow along the polar direction of the piezo actuators (R_{xx}), along which direction the strain was measured by the gauge. For one sample (x = 0.68), an additional crystal was mounted at 90° rotated according to the polar direction (R_{yy}). More details are described in **Section 3.3**. The sample resistance was collected with a combination of a high-precision current source and a nanovoltage meter. Because of the very large RRR (R_{300K}/R_0) values of the samples, special care was taken to avoid a temperature drift effect, and the electric current was set in an alternating positive/negative manner to avoid artifact.

We point out that noisy and irreproducible elastoresistance results can be acquired if DuPont® 4922N silver paint is used for making contacts to the samples. On the other hand, samples contacted with EPO-TEK® H20E epoxy or directly tin-soldering gave perfectly overlapping results. Given that DuPont® 4922N silver paint is widely used for transport measurements and is indeed suitable for elastoresistance experiments of other materials (for example) the $LaFe_{1-x}Co_xAsO$ series [12], we have no idea why it does not work for heavily hole-doped $Ba_{1-x}K_xFe_2As_2$ crystals. In this work, the presented data were collected by using the H20E epoxy. To avoid sample degradation, the epoxy was cured inside an Ar-glove box. A similar silver paint contact problem of $K/Rb/CsFe_2As_2$ crystals was also noticed by another group [29].

3 RESULTS AND DISCUSSIONS

3.1 Elastoresistance Measurement

The elastoresistance measured along the [110] direction of the KFe_2As_2 single crystal is shown in **Figure 1**. The sample resistance closely followed the strain change of the piezo actuator when the voltage across the piezo actuator is tuned. As presented in **Figure 1B**, the relationship between resistance change ($\Delta R/R$) and strain ($\Delta L/L$) is linear. This fact ensures that our experiments were performed in the small strain limit. In such a case, the elastoresistance χ^{er}, defined as the ratio between $\Delta R/R$ and the strain, acts as a measurement of the nematic susceptibility [10]. It is worthwhile to note that χ^{er} in KFe_2As_2 is positive (sample under tension yields higher resistance), consistent with the previous reports [27, 28] and opposite to that of $BaFe_2As_2$ [10]. It is to be noted that sign reversal of the elastoresistance was reported to occur in the underdoped region [33].

3.2 Elastoresistance of $K/Rb/CsFe_2As_2$

We start by showing our $\chi^{er}(T)$ data measured along the [110] direction ($\chi^{er}_{[110]}$) for a set of $(K/Rb/Cs)Fe_2As_2$ crystals. As shown in **Figure 2**, all the $\chi^{er}_{[110]}(T)$ curves follow a divergent behavior over the whole temperature range. A Curie–Weiss (CW) fit

$$\chi^{er} = \chi_0 + \frac{\lambda/a_0}{T - T^{nem}} \quad (1)$$

can record the data. A slight deviation can be discriminated at low temperature, which is typical for elastoresistance data and is

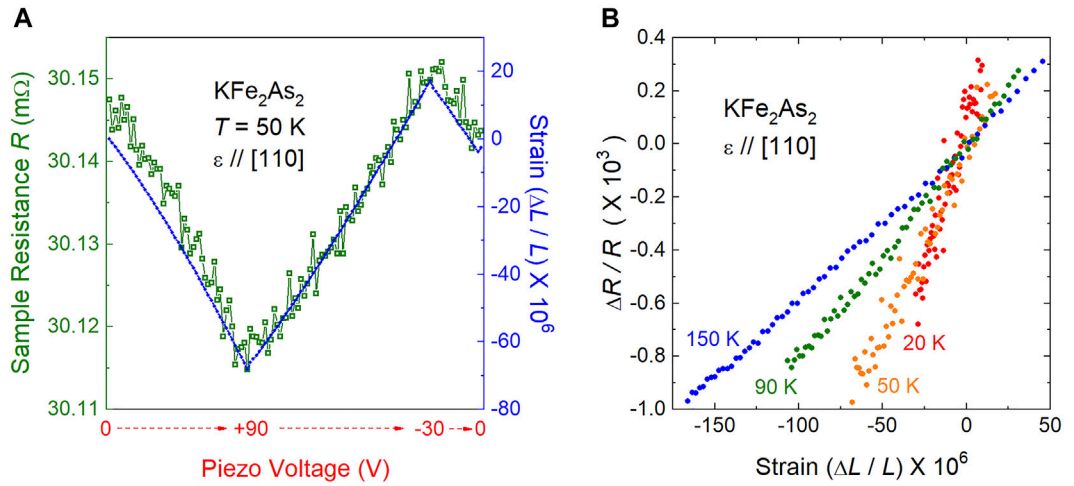

FIGURE 1 | Representative example of elastoresistance under strain for KFe_2As_2. **(A)** Resistance and strain change according to the voltage applied across the piezo actuator at a fixed temperature T = 50 K. The strain was applied along the [110] direction. **(B)** Change of resistance $\Delta R/R$ as a function of strain $\Delta L/L$ at several temperatures.

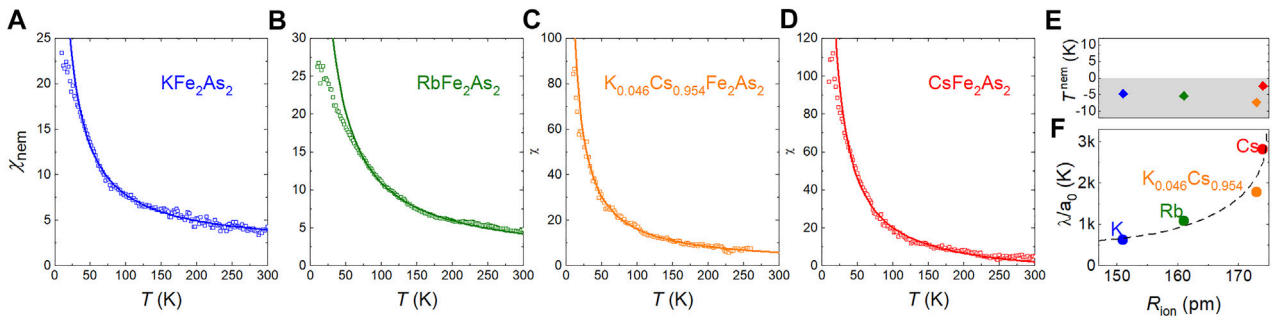

FIGURE 2 | Temperature dependence of elastoresistance $\chi^{er}_{[110]}$ for **(A)** KFe_2As_2, **(B)** $RbFe_2As_2$, **(C)** $K_{0.046}Cs_{0.095}Fe_2As_2$, and **(D)** $CsFe_2As_2$. Solid lines are CW-fit of the data (see text). The fit parameters T^{nem} and λ/a_0 are summarized in **(E,F)**, respectively. The dotted line in **(F)** is a guide to the eye.

understood as a disorder effect [13]. It is to be noted that the amplitude of the elastoresistance grows substantially from KFe_2As_2 to $CsFe_2As_2$, nearly 5-fold at 30 K. The extracted parameters from the CW fit are shown in **Figures 2E,F**. While the amplitude term shows a diverging trend, the T^{nem} of all four samples is of a very small negative value, which practically remains unchanged if experimental and fit uncertainties are taken into account, which is at odds with a possible nematic criticality in this isovalent-doping direction. The enhanced $\chi^{er}_{[110]}$ might be a result of a presumptive QCP of an unknown kind or a coherence–incoherence crossover [34–36]. These cannot be discriminated by our technique and thus are beyond the scope of this report.

3.3 Elastoresistance of Overdoped $Ba_{1-x}K_xFe_2As_2$

Next, we present a set of $\chi^{er}(T)$ data of five overdoped $Ba_{1-x}K_xFe_2As_2$ ($0.55 \leq x \leq 1$) across the Lifshitz point. The elastoresistance, measured only for the R_{xx} direction, as has been performed regularly in many reports [10, 12, 14], has been argued to be inconclusive for the end members (K/Rb/Cs)Fe_2As_2, as a result of the dominating A_{1g} contribution, instead of a B_{2g} (or B_{1g}) component which is related to nematicity [28, 29]. However, such complexities are ruled out by taking R_{yy} into account for calculating $\chi^{er}(T)$ for one representative example x = 0.68 (**Figure 3B**). The $\chi^{er}(T)$ curves calculated by the two different methods match well.

After checking the potential A_{1g} contribution to χ^{er} for a doping level close to the Lifshitz transition, we turn now to the data. As shown in **Figure 3**, the $\chi^{er}_{[110]}(T)$ curves of $Ba_{1-x}K_xFe_2As_2$ also follow a CW-like feature. One can see a clear dip at around 50 K in **Figure 3A** for the x = 0.55 sample. In some reports [27], such a feature was taken as a signal for a nematic order. Since no other ordering transition (structural, magnetic, and so on) has been ever reported in this doping range, we refrain from claiming an incipient nematic order solely based

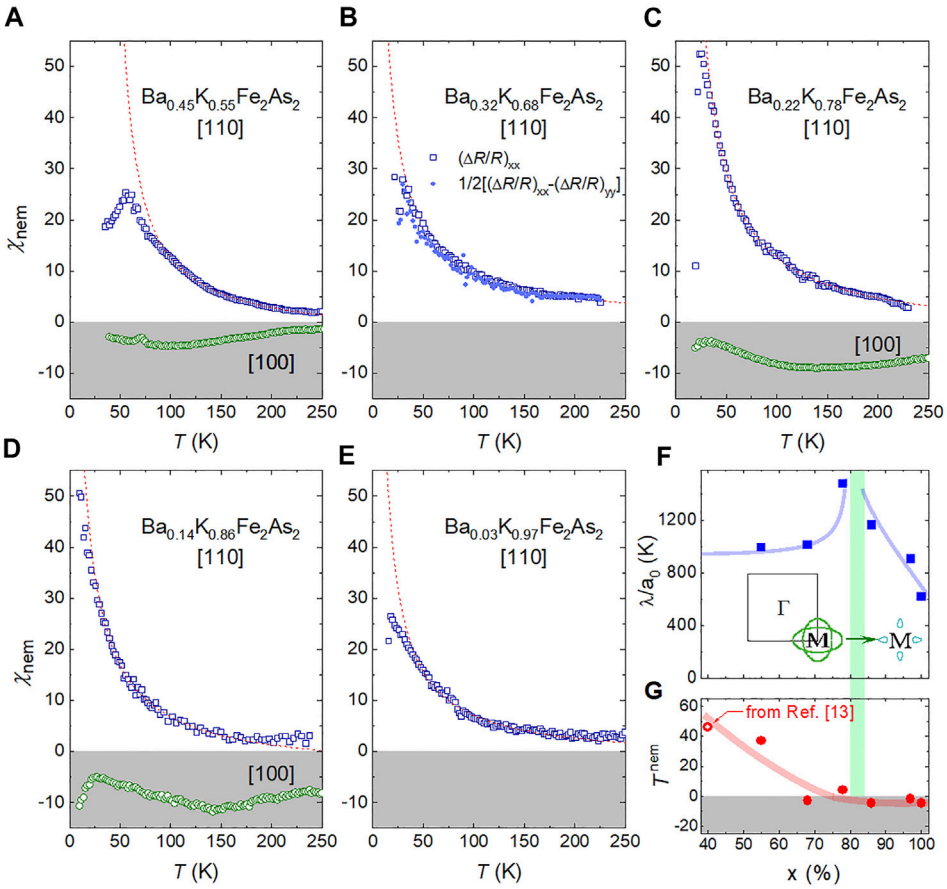

FIGURE 3 | Doping evolution of the elastoresistance in overdoped $Ba_{1-x}K_xFe_2As_2$. χ^{er} measured along the [110] direction is presented in the upper panels for $Ba_{1-x}K_xFe_2As_2$ single crystals with **(A)** $x = 0.55$, **(B)** $x = 0.68$, **(C)** $x = 0.78$, **(D)** $x = 0.86$, and **(E)** $x = 0.97$. The red dashed lines are CW-fit to the data. χ^{er} was also measured along the [100] direction for three of the samples. The data are presented in the lower panels of **(A)** and **(C,D)**. In panel **(B)**, χ^{er} extracted by using both $(\Delta R/R)_{xx}$ and $(\Delta R/R)_{yy}$ (filled light blue circles) and $(\Delta R/R)_{xx}$ (open blue squares) shows indistinguishable results. A doping dependence of the fit parameters is displayed in **(F)** λ/a_0 and **(G)** T^{nem} of the [110] $\chi^{er}_{[110]}$ data. The thick lines are a guide to the eye. A Lifshitz transition around $x = 0.8$ is highlighted by the green bar. Hole pockets around the M point of the Brillouin zone transform into electron lobes across the Lifshitz point [2]. T^{nem} at $x = 0.4$ is extracted from Ref. [13].

on such a feature. This might be equally well-explained by different origins. However, we also cannot exclude its possibility.

On the other hand, we measured χ^{er} along the [100] direction ($\chi^{er}_{[100]}$) for several samples. They are shown in the shaded panels of **Figure 3**. All of them are negative and small in amplitude, and none of them shows a CW-like feature. Such an observation is incompatible with the existence of B_{1g} nematicity in the heavily doped $Ba_{1-x}K_xFe_2As_2$ series, which is in sharp contrast to what is reported for the closely related $Ba_{1-x}Rb_xFe_2As_2$ series [27, 37, 38]. As a result, the so-called XY-nematicity is clearly ruled out in the $Ba_{1-x}K_xFe_2As_2$ series.

One remarkable feature, however, that can be safely concluded is that the amplitude of $\chi^{er}_{[110]}$ has a clear tendency to peak around $x = 0.8$, close to the Lifshitz transition. This becomes clearer in **Figure 3F**, where the CW fit parameters are plotted against the doping level. The question is why $\chi^{er}_{[110]}$ is increased at the Lifshitz transition? A nematic QCP is a potential explanation. However, as **Figure 3G** shows, T^{nem} drops from ~ 45 K of the $x = 0.4$ (optimal-doped) to ~ 0 K at the Lifshitz transition. Further doping does not drive T^{nem} to the more negative side within our experimental resolution. This is not typical QCP behavior. Moreover, since T_c across the Lifshitz transition is quite smooth, it seems not to be boosted by pertinent potential nematic fluctuations. Furthermore, three-point bending experiments did not show any anomaly in this doping range [39]. All these facts seem to be incompatible with the more understood nematic QCP in the electron-doped side [40]. Hence, if it is a nematic QCP, novel mechanisms need to be invoked. This motivated us to seek for alternative explanations for enhanced χ^{er} in heavily doped $Ba_{1-x}K_xFe_2As_2$. In the following section, we propose a conventional argument based on the small pocket effect, exempting from invoking a QCP to exist at the Lifshitz transition.

3.4 Theory for Enhanced Elastoresistance at the Lifshitz Transition

To study the effect of a Lifshitz transition to elastoresistance, we have calculated this quantity based on a minimal model of

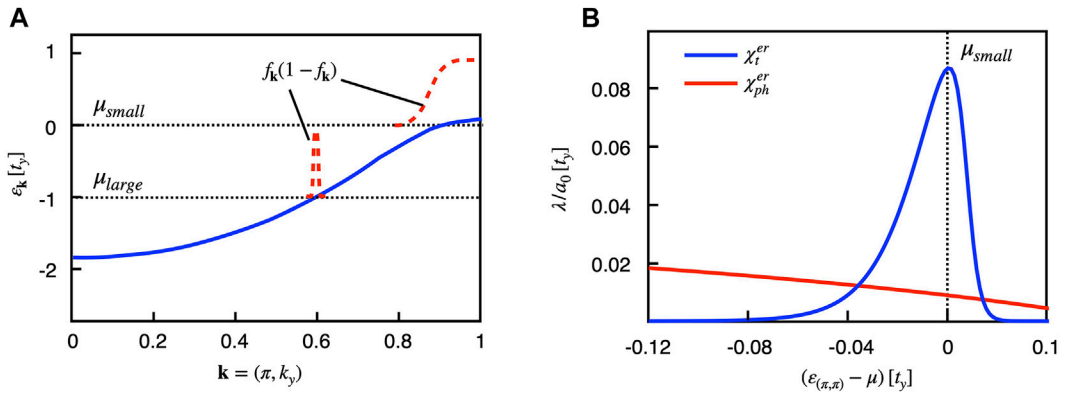

FIGURE 4 | Theoretical consideration of the elastoresisitivity. **(A)** Dispersion of the hole-like band leading to a very small hole pocket around the point (π, π) when the chemical potential μ_{small} (upper dotted line) is placed near the Lifshitz point. The range of momentum vectors contributing to the elastoresisitivity arising from the Fermi function is schematically shown by the dashed lines. A much larger hole pocket is indicated by a lower value of the chemical potential μ_{large} (lower dotted line). **(B)** Calculated parts of the elastoresistivity according to **Eq. 3**. Around the Lifshitz point μ_{small} the first-order part χ_t^{er} dominates the second-order part which is, however, the most important contribution for μ away from the Lifshitz point.

iron-based superconductors [41] with a very small Fermi surface. The corresponding dispersion which was used is shown in **Figure 4A** for the normal state along a cut (π, k_y). We considered the two orbital models in Ref. [41] with the same hopping matrix elements but having set the nematic interaction equal to a very small value. Thus, the nematic interaction accounts here only for the temperature dependence of the susceptibility according to the Curie–Weiss law. Moreover, we introduced a very small lattice distortion in the x direction which is coupled with the electron system. Using the first-order perturbation theory with respect to this coupling (linear response), we then calculated the elastoresistivity. We have considered two different cases of the coupling between distortion and electrons (strength g): (i) The conventional coupling with the local electron density (electron–phonon coupling), where we denote the corresponding response with χ_{ph}. (ii) A direct coupling of the distortion with the hopping matrix element t_x in the x direction. The corresponding response is denoted by χ_t.

$$\begin{aligned}\chi_t &\propto g \lim_{\Delta t_x \to 0} \frac{\sigma_{xx}^{-1}(t_x+\Delta t_x)-\sigma_{yy}^{-1}(t_x+\Delta t_x)}{\Delta t_x}\\ \chi_{ph} &\propto \frac{1}{N}\sum_{\mathbf{k}}\left(\frac{g}{\omega+\varepsilon_{\mathbf{k}}-\varepsilon_{\mathbf{k}+\mathbf{q}}}\right)^2 \frac{f_{\mathbf{k}}-f_{\mathbf{k}+\mathbf{q}}}{\varepsilon_{\mathbf{k}+\mathbf{q}}-\varepsilon_{\mathbf{k}}}.\end{aligned} \tag{2}$$

Here, t_x is the hopping matrix element in the x direction and σ_{xx}, σ_{yy} are the conductivities in the x and y directions [41]. The phonon energy ω in χ_{ph}^{er} is in general renormalized by the coupling to the electrons and becomes soft for a particular mode if the system is near a structural phase transition[42, 43]. The electron dispersion $\varepsilon_{\mathbf{k}}$ considered here is shown in **Figure 4A**. The function $f_{\mathbf{k}}$ is the Fermi distribution with respect to $\varepsilon_{\mathbf{k}}$. Thus, for most systems investigated, this term dominates χ^{er}. It is to be noted how magnetic fluctuations impact the phonons and the nematicity has been investigated [9, 16].

Figure 4B shows the two parts χ_t^{er} and χ_{ph}^{er} which were calculated separately as a function of the chemical potential μ to simulate different doping values. To compare with **Figure 3F**, we extracted the temperature behavior according to **Eq. 2** and plotted the calculated value λ/a_0 in energy units of t_y. It is seen that the first-order part χ_t^{er} dominates the second-order part only in the narrow range of μ, where the Fermi surface around (π, π) becomes very small. Thus, only when the system has very small Fermi surfaces, as in the case of $Ba_{1-x}K_xFe_2As_2$ at the Lifshitz transition, the term χ_t^{er} becomes important. However, it is also seen that if the chemical potential is chosen away from the Lifshitz point corresponding to a proper doping, the second-order part χ_{ph}^{er} is mostly important as expected.

The enhancement of χ_t^{er} in the presence of a very small Fermi surface can be explained by the existence of low-energy excitations in a relatively wide range of momentum vectors. Since the conductivities are proportional to Fermi distribution functions $f_{\mathbf{k}}$ as follows

$$\sigma_{ii} \propto \sum_{\mathbf{k}} \left(\frac{\partial \varepsilon_{\mathbf{k}}}{\partial k_i}\right)^2 f_{\mathbf{k}}(1-f_{\mathbf{k}}), \tag{3}$$

we find that at low temperature, if the Fermi surface is small, the momentum range $\mathbf{k}$, where $f_{\mathbf{k}}(1-f_{\mathbf{k}})$ is non-zero, is much larger because of the tendency of the band to rapidly change the Fermi surface topology near the Lifshitz transition (compare the red dashed lines in **Figure 4A**) than for a usual Fermi surface.

4 CONCLUSION

To summarize, we reported that a CW-like $\chi^{er}(T)$ is observed for all kinds of heavily hole-doped 122s. There is an unexpected

enhancement of the elastoresistance around the Lifshitz transition. We explained it as a small Fermi pocket effect on the nematicity. We expect that our explanation of an alternative contribution to the enhanced elastoresistance other than a nematic QCP will be considered in other systems, in particular for those with small Fermi pockets.

DATA AVAILABILITY STATEMENT

The raw data supporting the conclusions of this article will be made available by the authors, without undue reservation.

AUTHOR CONTRIBUTIONS

IM, SA, VG, KK, and C-HL prepared the samples. XH, FC, and MB performed the experiments. SS proposed the theoretical model. CH and BB supervised the study. XH, SS, FC, and CH analyzed the data and wrote the manuscript with input from all authors.

FUNDING

This work has been supported by the Deutsche Forschungsgemeinschaft (DFG) through SFB 1143 (Project No. 247310070), through the Research Projects CA 1931/1-1 (FC) and SA 523/4-1 (SA). SS acknowledges funding by the Deutsche Forschungs gemeinschaft *via* the Emmy Noether Program ME4844/1-1 (project id 327807255). This project has received funding from the European Research Council (ERC) under the European Union's Horizon 2020 Research and Innovation Program (grant agreement No. 647276-MARS-ERC-2014-CoG).

ACKNOWLEDGMENTS

We would like to thank Anna Böhmer, Ian Fisher, Suguru Hosoi, Rüdiger Klingeler, Christoph Meingast, Jörg Schmalian, Christoph Wuttke, Paul Wiecki, and Liran Wang for helpful discussions. We would like to thank Christian Blum and Silvia Seiro for their technical support.

REFERENCES

1. Chen X, Dai P, Feng D, Xiang T, Zhang FC. Iron-based High Transition Temperature Superconductors. *Natl.Sci.Rev.* (2014) 1:371–95. doi:10.1093/nsr/nwu007
2. Xu N, Richard P, Shi X, van Roekeghem A, Qian T, Razzoli E. Possible Nodal Superconducting gap and Lifshitz Transition in Heavily Hole-Doped $Ba_0._1K_{0.9}Fe_2As_2$ *Phys.Rev.B* (2013) 88:220508. doi:10.1103/PhysRevB.88.220508
3. Malaeb W, Shimojima T, Ishida Y, Okazaki K, Ota Y, Ohgushi K, et al. Abrupt Change in the Energy gap of Superconducting $Ba_{1-x}K_xFe_2As_2$ Single Crystals with Hole Doping. *Phys.Rev.B* (2012) 86:165117. doi:10.1103/PhysRevB.86.165117
4. Hong XC, Wang AF, Zhang Z, Pan J, He LP, Luo XG, et al. Doping Evolution of the Superconducting Gap Structure in Heavily Hole-Doped $Ba_{1-x}K_xFe_2As_2$: a Heat Transport Study. *Chin.Phys.Lett.* (2015) 32:127403. doi:10.1088/0256-307X/32/12/127403
5. Grinenko V, Materne P, Sarkar R, Luetkens H, Kihou K, Lee CH, et al. Superconductivity with Broken Time-Reversal Symmetry in Ion-Irradiated $Ba_{0.27}K_{0.73}Fe_2As_2$ Single Crystals. *Phys.Rev.B* (2017) 95:214511. doi:10.1103/PhysRevB.95.214511
6. Grinenko V, Sarkar R, Kihou K, Lee CH, Morozov I, Aswartham S, et al. Superconductivity with Broken Time-Reversal Symmetry inside a Superconducting *S*-Wave State. *Nat.Phys.* (2020) 16:789. doi:10.1038/s41567-020-0886-9
7. Grinenko V, Weston D, Caglieris F, Wuttke C, Hess C, Gottschall T, et al. State with Spontaneously Broken Time-Reversal Symmetry above the Superconducting Phase Transition. *Nat.Phys.* (2021) 17:1254. doi:10.1038/s41567-021-01350-9
8. Fisher IR, Degiorgi L, Shen ZX. In-plane Electronic Anisotropy of Underdoped '122' Fe-Arsenide Superconductors Revealed by Measurements of Detwinned Single Crystals. *Rep.Prog.Phys.* (2011) 74:124506. doi:10.1088/0034-4885/74/12/124506
9. Fernandes RM, Chubukov AV, Schmalian J. What Drives Nematic Order in Iron-Based Superconductors? *Nat.Phys.* (2014) 10:97. doi:10.1038/nphys2877
10. Chu JH, Kuo HH, Aanlytis JG, Fisher IR. Divergent Nematic Susceptibility in an Iron Arsenide Superconductor. *Science* (2012) 337:710. doi:10.1126/science.1221713
11. Hosoi S, Matsuura K, Ishida K, Wang H, Mizukami Y, Watashige T, et al. Nematic Quantum Critical point without Magnetism in $FeSe_{1-x}S_x$ Superconductors. *Proc.Natl.Acad.Sci.U.S.A.* (2016) 113:8139. doi:10.1073/pnas.1605806113
12. Hong XC, Caglieris F, Kappenberger R, Wurmehl S, Aswartham S, Scaravaggi F, et al. Evolution of the Nematic Susceptibility in $LaFe_{1-x}Co_xAsO$. *Phys.Rev.Lett.* (2020) 125:067001. doi:10.1103/PhysRevLett.125.067001
13. Kuo HH, Chu JH, Palmstrom JC, Kivelson SA, Fisher IR. Ubiquitous Signatures of Nematic Quantum Criticality in Optimally Doped Fe-Based Superconductors. *Science* (2016) 52:958. doi:10.1126/science.aab0103
14. Gu YH, Liu ZY, Xie T, Zhang WL, Gong DL, Hu D, et al. Unified Phase Diagram for Iron-Based Superconductors. *Phys.Rev.Lett.* (2017) 119:157001. doi:10.1103/PhysRevLett.119.157001
15. Terashima T, Matsushita Y, Yamase H, Kikugawa N, Abe H, Imai M, et al. Elastoresistance Measurements on $CaKFe_4As_4$ and $KCa_2Fe_4As_4F_2$ with the Fe Site of C_{2v} Symmetry. *Phys.RevB* (2020) 102:054511. doi:10.1103/PhysRevB.102.054511
16. Fernandes RM, Schmalian J. Manifestations of Nematic Degrees of freedom in the Magnetic, Elastic, and Superconducting Properties of the Iron Pnictides. *Supercond.Sci.Technol.* (2012) 25:084005. doi:10.1088/0953-2048/25/8/084005
17. Lederer S, Schattner Y, Berg E, Kivelson SA. Enhancement of Superconductivity Near a Nematic Quantum Critical Point. *Phys.Rev.Lett.* (2015) 114:097001. doi:10.1103/PhysRevLett.114.097001
18. Labat D, Paul I. Pairing Instability Near a Lattice-Influenced Nematic Quantum Critical point. *Phys.Rev.B* (2017) 96:195146. doi:10.1103/PhysRevB.96.195146
19. Maslov DL, Chubukov AV. Fermi Liquid Near Pomeranchuk Quantum Criticality. *Phys.Rev.B* (2010) 81:045110. doi:10.1103/PhysRevB.81.045110
20. Tafti FF, Juneau-Fecteau A, Delage M-E, René de Cotret S, Reid J-P, Wang AF, et al. Sudden Reversal in the Pressure Dependence of T_c in the Iron-Based Superconductor KFe_2As_2. *Nat.Phys.* (2013) 9:349. doi:10.1038/nphys2617
21. Wang YQ, Lu PC, Wu JJ, Liu J, Wang XC, Zhao JY, et al. Phonon Density of States of Single-crystal $SrFe_2As_2$ across the Collapsed Phase Transition at High Pressure. *Phys.Rev.B* (2016) 94:014516. doi:10.1103/PhysRevB.94.014516
22. Ptok A, Sternik M, Kapcia KJ, Piekarz P. Structural, Electronic, and Dynamical Properties of the Tetragonal and Collapsed Tetragonal Phases of KFe_2As_2. *Phys.Rev.B* (2019) 99:134103. doi:10.1103/PhysRevB.99.134103
23. Ptok A, Kapcia KJ, Cichy A, Oleś AM, Piekarz P. Magnetic Lifshitz Transition and its Consequences in Multi-Band Iron-Based Superconductors. *Sci.Rep.* (2017) 7:41979. doi:10.1038/srep41979
24. Li J, Zhao D, Wu YP, Li SJ, Song DW, Zheng LX, et al. *Reemergeing Electronic Nematicity in Heavily Hole-Doped Fe-Based Superconductors* (2016). arXiv:1611.04694.

25. Liu X, Tao R, Ren MQ, Chen W, Yao Q, Wolf T, et al. Evidence of Nematic Order and Nodal Superconducting gap along [110] Direction in $RbFe_2As_2$. *Nat.Commun.* (2019).
26. Fernandes RM, Orth PP, Schmalian J. Intertwined Vestigial Order in Quantum Materials: Nematicity and beyond. *Annu.Rev.Condens.MatterPhys.* (2019) 10: 133. doi:10.1146/annurev-conmatphys-031218-013200
27. Ishida K, Tsujii M, Hosoi S, Mizukami Y, Ishida S, Iyo A, et al. Novel Electronic Nematicity in Heavily Hole-Doped Iron Pnictide Superconductors. *Proc.Natl.Acad.Sci.U.S.A.* (2020) 117:6424. doi:10.1073/pnas.1909172117
28. Wiecki P, Haghighirad AA, Weber F, Merz M, Heid R, Böhmer AE. Dominant In-Plane Symmetric Elastoresistance in $CsFe_2As_2$. *Phys.Rev.Lett.* (2020) 125: 187001. doi:10.1103/PhysRevLett.125.187001
29. Wiecki P, Frachet M, Haghighirad AA, Wolf T, Meingast C, Heid R, et al. Emerging Symmetric Strain Response and Weakening Nematic Fluctuations in Strongly Hole-Doped Iron-Based Superconductors. *Nat.Commun.* (2021) 12:4824. doi:10.1038/s41467-021-25121-5
30. Aswartham S, Abdel-Hafiez M, Bombor D, Kumar M, Wolter AUB, Hess C, et al. Hole Doping in $BaFe_2As_2$: The Case of $Ba_{1-x}Na_xFe_2As_2$ Single Crystals. *Phys.Rev.B* (2012) 85:224520. doi:10.1103/PhysRevB.85.224520
31. Abdel-Hafiez M, Aswartham S, Wurmehl S, Grinenko V, Hess C, Drechsler S-L, et al. Specific Heat and Upper Critical fields in KFe_2As_2 Single Crystals. *Phys.Rev.B* (2012) 85:134533. doi:10.1103/PhysRevB.85.134533
32. Moroni M, Prando G, Aswartham S, Morozov I, Bukowski Z, Büchner B, et al. Charge and Nematic Orders in AFe_2As_2 (A = Rb, Cs) Superconductors. *Phys.Rev.B* (2019) 99:235147. doi:10.1103/PhysRevB.99.235147
33. Blomberg EC, Tanatar MA, Fernandes RM, Mazin II, Shen B, Wen HH, et al. Sign-reversal of the In-Plane Resistivity Anisotropy in Hole-Doped Iron Pnictides. *Nat.Commun.* (2013) 4:1914. doi:10.1038/ncomms2933
34. Eilers F, Grube K, Zocco DA, Wolf T, Merz M, Schweiss P, et al. Strain-Driven Approach to Quantum Criticality in AFe_2As_2 with A=K, Rb, and Cs. *Phys.Rev.Lett.* (2016) 116:237003. doi:10.1103/PhysRevLett.116.237003
35. Zhang ZT, Dmytriieva D, Molatta S, Wosnitza J, Khim S, Gass S, et al. Increasing Stripe-type Fluctuations in AFe_2As_2 (A=K, Rb, Cs) Superconductors Probed by ^{75}As NMR Spectroscopy. *Phys.Rev.B* (2018) 97: 115110. doi:10.1103/PhysRevB.97.115110
36. Hardy F, Böhmer AE, Aoki D, Burger P, Wolf T, Schweiss P, et al. Evidence of Strong Correlations and Coherence-Incoherence Crossover in the Iron Pnictide Superconductor KFe_2As_2. *Phys.Rev.Lett.* (2013) 111:027002. doi:10.1103/PhysRevLett.111.027002
37. Onari S, Kontani H. Origin of Diverse Nematic Orders in Fe-Based Superconductors: 45° Rotated Nematicity in AFe_2As_2 (A=Cs,Rb). *Phys.Rev.B* (2019) 100:020507. doi:10.1103/PhysRevB.100.020507
38. Borisov V, Fernandes RM, Valentí R. Evolution from B_{2g} Nematics to B_{1g} Nematics in Heavily Hole-Doped Iron-Based Superconductors. *Phys.Rev.Lett.* (2019) 123:146402. doi:10.1103/PhysRevLett.123.146402
39. Böhmer AE, Burger P, Hardy F, Wolf T, Schweiss P, Fromknecht R, et al. Nematic Susceptibility of Hole-Doped and Electron-Doped $BaFe_2As_2$ Iron-Based Superconductors from Shear Modulus Measurements. *Phys.Rev.Lett.* (2014) 112:047001. doi:10.1103/PhysRevLett.112.047001
40. Fernandes RM, VanBebber LH, Bhattacharya S, Chandra P, Keppens V, Mandrus D, et al. Effects of Nematic Fluctuations on the Elastic Properties of Iron Arsenide Superconductors. *Phys.Rev.Lett.* (2010) 105:157003. doi:10.1103/PhysRevLett.105.157003
41. Wuttke C, Caglieris F, Sykora S, Steckel F, Hong X, Ran S, et al. *Ubiquitous Enhancement of Nematic Fluctuations across the Phase Diagram of Iron Based Superconductors Probed by the Nernst Effect*. arXiv:2202.00485.
42. Sykora S, Hübsch A, Becker KW. Dominant Particle-Hole Contributions to the Phonon Dynamics in the Spinless One-Dimensional Holstein Model. *Europhys.Lett.* (2006) 76:644. doi:10.1209/epl/i2006-10327-x
43. Sykora S, Hübsch A, Becker KW. Generalized Diagonalization Scheme for many-particle Systems. *Phys.Rev.B* (2020) 102:165122. doi:10.1103/PhysRevB.102.165122

Conflict of Interest: The authors declare that the research was conducted in the absence of any commercial or financial relationships that could be construed as a potential conflict of interest.

Publisher's Note: All claims expressed in this article are solely those of the authors and do not necessarily represent those of their affiliated organizations, or those of the publisher, the editors, and the reviewers. Any product that may be evaluated in this article, or claim that may be made by its manufacturer, is not guaranteed or endorsed by the publisher.